Journal of Thermal Analysis and Calorimetry (2021) 145:635–647
https://doi.org/10.1007/s10973-020-10071-9

Exergy analyzing of a horizontal-axis wind turbine in different conditions based on the BEM method

Mohammad Ajam[1] · Hamid Mohammadiun[1] · Mohammad Hossein Dibaee[1] · Mohammad Mohammadiun[1]

Received: 26 April 2020 / Accepted: 13 July 2020 / Published online: 4 August 2020

Abstract

In this study, a horizontal-axis wind turbine based on the first and second laws of thermodynamics in different wind speeds and pitch angles is analyzed. The blade element momentum (BEM) theory coupled by the exergy equations was implemented to model the wind turbine at wind speeds from 6 to 15 m s^{-1} and three different pitch angles 5°, 10°, and 20°. The aim of this study was to evaluate the effects of metrological variables such as wind speed, temperature, pressure, and relative humidity on the exergy efficiency of the wind turbine in different pitch angles. It is found out that the wind turbine has been affected more by wind speed compared to other metrological parameters and the highest exergy efficiency is 42.8% at wind speed 12 m s^{-1} and pitch angle 5°. Also, it is shown that the rising of pressure changes and relative humidity decreases the exergy efficiency for all wind speeds and pitch angles. Increasing the relative humidity from 0.001 to 0.015 and pressure changes from 100 to 240 pa can decrease the exergy efficiency 1.76% and 1.26% at the wind speed of 8 m s^{-1} and pitch angle of 20°, respectively. In contrast, temperature has a positive impact on the exergy efficiency in the same condition and is able to increase the exergy efficiency 2% by changing from 5 to 35 °C at wind speed of 8 m s^{-1} and the pitch angle of 5°.

Keywords Exergy analysis · Energy analysis · Exergy flow · Exergy destruction · Wind exergy

List of symbols

a	Axial induction factor
a'	Tangential induction factor
c	Chord (m)
C_d	Drag coefficient
C_l	Lift coefficient
c_p	Specific heat (kJ kg^{-1} K^{-1})
CP	Power coefficient
D	Drag force (N)
Ex	Exergy (W)
F	Force (N)
f	Prandtl's tip loss
I	Irreversibility (kW)
ke	Kinetic energy (J)
L	Lift force (N)
m	Mass (kg)
$\dot{m}$	Mass flow rate (kg s^{-1})
P	Pressure (kPa)
R	Gas constant (kJ kg^{-1} K^{-1}) and radius (m)
r	Local radius (m)
T	Temperature (k)
t	Time (s)
TSR	Tip speed ratio
v	Velocity (m s^{-1})
w_{i2}	Tangential induced velocity
W	Work (J) and relative velocity (m s^{-1})

Greek letters

α	Angle of attack (rad)
β	Pitch angle (rad)
η	Energy efficiency
Ω	Rotor speed (rad s^{-1})
ρ	Density (kg m^{-3})
σ'	Solidity
φ	Flow angle (rad)
Ψ	Exergy efficiency
ϖ	Specific humidity

Subscripts

des	Exergy destruction
ph	Physical
0	Ambient
1	Inlet

✉ Hamid Mohammadiun
hmohammadiun@yahoo.com

Mohammad Ajam
mohammad.ajam7171@gmail.com

[1] Department of Mechanical Engineering, Shahrood Branch, Islamic Azad University, Shahrood, Iran

2	Outlet
out	Output
avg	Average

Introduction

Using fossil fuels in order to meet the energy demand of the world has brought a lot of environmental problems such as global warming and air pollution [1, 2]. Moreover, the resources of these fuels are limited and the energy crisis has been becoming an important issue in recent decades [3]. Therefore, several strategies like using efficient hybrid energy systems or renewable energy resources should be applied to decrease the consequences of fossil fuels consumption [4, 5].

Renewable energy resources like wind and solar energy have been known as the types of energy that are clean and have the lowest impact on the environment compared to fossil fuels [6–8]. With the rapid advancement of wind turbine technology and its expansion in the energy production portfolio of countries, the need to study the performance of wind turbines in different climatic conditions has become very important for wind energy engineers [9]. The study of some thermodynamic variables of wind flow has not yet been fully investigated in the wind turbine's operation. In most studies, the power factor or the wind turbine energy efficiency ratio is considered to be the ratio of the power extracted from the wind turbine to the kinetic energy of the wind that is in contact with the rotor plate (first law of thermodynamics concept). Since this assumption does not take into account the other wind flow's characteristics such as temperature, humidity, and pressure difference, this assumption will not be accurate enough to analyze the efficiency of a wind turbine. Therefore, studying the wind turbine based on the second law of thermodynamics (exergy analysis) is an alternative way to reach a comprehensive insight into the wind turbine's performance in different conditions.

Exergy analysis is one of the important tools for evaluating renewable energy cases and hybrid systems in different scenarios [10, 11]. This key not only gives a clear picture of the effects of each variable on the system but also is a good way to analyze the system economically in the energy markets [12–15]. For example, Chunpeng used various scenarios based on wind energy scopes to reach a sustainable and clean energy in the multigenerational systems, and it was shown the effect of wind energy on electricity price reduction [16]. Similarly, Maleki proposed a cost-effective system using wind energy and demonstrated the effect of wind in cost and efficiency of the system [17]. Barhoumi analyzed the different resources of renewable energy in Saudi Arabia and finally explained the importance of wind and solar energy in this country for the future [18]. In these studies, the importance of wind energy resources for the future of the energy market based on the exergy analysis is shown. The exergy concept can be used to analyze the wind turbine in a hybrid system. Koroneos studied the exergy efficiency of a renewable system including a wind turbine to determine the electricity production of a hybrid system [19]. He concluded that even though wind flow has much more influence on energy and exergy efficiencies, the effects of other metrological variables are important in the calculation. Khalilzadeh employed the exergy and thermoeconomic concept to assess using waste heat from a wind turbine for desalination [20]. It was shown that this idea seems to be useful as it increases the exergy efficiency of the integrated system by 7.34%. Also, regarding the cost of potable water, the average rate of return and payback period are predicted as 6.76% and 6.33 years, respectively. Similarly, Nematollahi proposed a novel method to use the heat waste of wind turbine into an organic Rankine cycle system and analyzed it based on the second law of thermodynamic [21]. Khosravi defined and assessed an off-grid hydrogen storage system combining solar panel and wind turbine, hydrogen production unit, and fuel cell. It was demonstrated that the average energy and exergy efficiencies of the wind turbine were 32% and 25%, respectively [22]. Mohammadi analyzed the exergy efficiency of a combined cooling, heating, and power system integrated with wind turbine and compressed air energy storage system [23]. The result of this study revealed that wind turbine and combustion chamber are the most important sources of the exergy destruction in this system.

In these researches, it was assumed that the wind turbine is a stable part of the systems and did not take into account the effect of the wind turbine's fluctuations caused by metrological variables changes on the system, while it is clear that changing the metrological variables in different conditions can affect the wind turbine's performance.

Aghbashlo compared the different exergy analysis methods used to model the efficiency of a wind farm in Iran and propose an accurate approach to assess a wind power plant under different conditions [24]. Ahmadi conducted an exergetic analysis on a vertical-axis wind turbine [25]. He modeled the entropy generation, and observed by increasing the entropy generation in the system that the output power produced by wind turbine drops dramatically. Baskut evaluated the impacts of meteorological parameters namely temperature, pressure differences, and humidity on the exergy efficiency of a wind site in Turkey [26].

In these cases, the results of the experimental data were used to model the wind turbines based on the second law of thermodynamics. But it should be mentioned that measuring the wind speed behind the rotor plan is very important to calculate the exergy flow in research, which is mostly calculated based on the kinetic energy changes; however, it is clear that wake production and irreversibility behind the

wind turbine affect the kinetic energy of the system. Therefore, using aerodynamic modeling can be a good way to model the wind turbine and calculate the wind speed in different zones. Pope uses the CFD simulation method to model 4 different wind turbines in different conditions [27]. He modeled two vertical-axis wind turbines and two horizontal-axis wind turbines and used different methods to measure the wind speed behind the wind turbines in order to show how much calculating the wind speed behind the wind turbine can affect the calculations. However, there is no experimental data for this research to validate the calculated results. Khanjari employed the blade element momentum (BEM) method to model the MEXICO wind turbine and study the effect of the yaw changes and roughness intensity [28, 29]. He demonstrated that the BEM theory is a trustable method to model a wind turbine to calculate exergy parameters. It was concluded that increasing the roughness intensity and the yaw angle will decrease the power production and the exergy efficiency dramatically. Moreover, it was shown that the effect of the pressure changes, temperature, and humidity of wind flow at the wind speed of 24 m s^{-1} on the exergy efficiency of the wind turbine but these effects were not fully studied in different wind speeds and pitch angles to show the effect of every single parameter on the wind turbine's performance.

In all cases, it was shown that the wind speed has had a significant effect on the exergy efficiency compared to the other metrological variables. But it was not shown the effect of each parameter on the exergy efficiency as a comprehensive study. On the other hands, they showed the effects of the metrological parameters in a constant wind speed and pitch angle, which will not give a clear understanding about these parameters.

In this study, the BEM theory is employed to model a 150 KW horizontal-axis wind turbine and then study the effect of temperature, pressure, and relative humidity in different wind speeds and pitch angles on the wind turbine performances based on the first and second laws of thermodynamics. The aim of this study is to show how much the metrological parameters can affect the exergy efficiency of the wind turbine in different wind speeds and pitch angles.

Materials and methods

Wind turbine energy analysis

Raising the wind turbine's efficiency is one of the hottest topics between scientists. Therefore, studying the wind turbine's performance in different conditions is vital in order to achieve this goal [29, 30]. With this said, aero-dynamical modeling of the wind turbine can help us to achieve a profound insight into the wind blades' reaction in different conditions before constructing them.

There are two distinct ways to simulate the wind turbine aerodynamically:

1. Modeling the wind turbine by using the blade element momentum (BEM) theory, this has a satisfactory prediction and needs less time to calculate the aerodynamic loads on the wind turbine compared to other methods [28, 31, 32].
2. Modeling of the wind turbine in computational fluid dynamics (CFD). It is governed by Navier–Stokes equations. This method is able to plot the different contours of the wind flow before and after the wind turbine but it is time-consuming. Also, the cost of wake simulation in this method is high [33–35].

Direct modeling (DM), which implements the exact geometry of the wind blades, is the common approach to simulate wind turbines in the CFD domain. Also, actuator disk (AD), actuator surface (AS), and actuator line (AL) are other methods in the CFD domain, coupling Navier–Stokes equations by BEM concept to eliminate the geometry of blades in the domain and decrease the time consumed by computers [33, 36, 37].

In order to apply the BEM code, airfoil characteristics are needed, which are mostly based on 2-dimensional (2D) measurements. Due to 3-dimensional (3D) effects, the BEM code will not able to predict a trustable result. Therefore, using the 3D aerofoil correction is a pivotal part of modeling [38].

Mahmoodi showed that an improved BEM model using 3D correction in the stall region has a more accurate prediction than AD simulation in the CFD domain [39]. Moreover, Kabir used the BEM method employing the 3D correction to evaluate the stall delay phenomenon for the NREL[1] Phase VI wind turbine having five radial locations. It was concluded that this has a good agreement with aerofoil characteristics distribution along the blade span and a good matching for aerodynamics load as well as power production [40]. Pinto studied the BEM theory to optimize the wind turbine's performance aerodynamically. He demonstrated that in order to reach an optimal operating condition for a wind turbine, all sections of blades have to operate at maximum lift-to-drag ratio [41].

Arramach implemented the BEM theory coupled by brake state model for NREL wind turbine to determine the axial and tangential induction factors in different tip speed ratios and studied the effect of radial flow along the blades

[1] National Renewable Energy Laboratory.

causing the centrifugal pumping on the wind turbine in both pre-stall and post-stall regions [42].

Another correction that has a considerable effect to reach a reliable prediction in BEM modeling is tip loss correction. Zhong implemented the tip loss correction for three wind turbines and concluded that this correction has a satisfactory agreement with experimental results in a wide range of tip speed ratios [43].

BEM theory

BEM theory combines both blade element theory and momentum theory to calculate the force on the wind turbine's blades. At first, this theory was used by Froude [44] later refined by Glauert [45].

By assuming the wind flow around the wind turbine is incompressible and axisymmetric, BEM theory is a good tool for understanding wind turbine aerodynamics [46]. In this study, the BEM method developed and described in detail by Glauert and Hansen is implemented [45, 47]. Each blade of the wind turbine is divided into several elements, and the performance of them is deduced by applying the momentum conservation principle [44, 48, 49].

A wind turbine rotating in each angular velocity generates a wake behind itself, which has a determinable impact on the flow upstream [50, 51]. Consequently, the wind speed before touching the blades $V1$ will be decreased by the wake induced velocity. It will be obtained by applying the momentum theorem in the axial direction [47].

$$V_1 = V_0(1-a) \tag{1}$$

That a is the axial induction factor.

Avoiding the breaking down of the integration process, a correction is used as Eq. (2) [52]

$$a = \begin{cases} (k+1)^{-1}, & a \le a_c \\ \frac{1}{2}\left(2 + k\left(1-2a_c\right) - \sqrt{\left(k\left(1-2a_c\right)+2\right)^2 + 4\left(k\cdot a_c^2\right)} - 1\right), & a \ge a_c \end{cases} \tag{2}$$

$$k = \frac{4f\sin\phi^2}{\sigma'\left(c_l\cos(\phi) + c_d\sin(\phi)\right)} \tag{3}$$

$$\sigma' = 3c/2\pi r \tag{4}$$

where k is an auxiliary function and $a_c = 0.3$ is the separation point of the thrust coefficient in the high axial induction factor, C_l and C_d are the lift and drag coefficient.

Also, the tip loss correction is used in this study is defined by following equation [47, 50].

$$f = \frac{2}{\pi}\arccos\left(e^{-\left(\frac{3(R-r)}{2r\sin\phi}\right)}\right) \tag{5}$$

f is Prandtl's tip loss correcting the turbine as a finite bladed rotor.

Moreover, there is a similar equation for the rotational speed [47, 50].

$$a' = \frac{w_{i2}}{\Omega} \tag{6}$$

where w_{i2} is the tangential induced velocity at the plane just before the rotor and a' is the tangential induction factor.

Other parameters like the angle of flow (ϕ) and the angle of attack (α) are followed by Eqs. 6 and 7 [47].

$$\phi = a\tan\left(\frac{V_0(1-a)}{r\Omega(1+a')}\right) \tag{7}$$

$$\alpha = \phi - \beta \tag{8}$$

Regarding Fig. 1, in order to calculate the power produced by wind turbine, the axial and tangential forces on a blade element should be:

In Fig. 1, V_o is incoming wind speed, Ω is angular velocity of the blade, r is local radius of the element, W is relative velocity, β is pitch angle, ϕ is flow angle, L and D are the induced lift and drag forces per blade length, respectively [47].

$$W = \sqrt{V_o^2(1-a)^2 + \Omega^2 r^2(1+a')^2} \tag{9}$$

$$L = \frac{1}{2}\rho W^2 C_l c, \quad C_l = f(r,\alpha) \tag{10}$$

$$D = \frac{1}{2}\rho W^2 C_d c, \quad C_d = g(r,\alpha) \tag{11}$$

$$dF_{ax} = L\cdot\cos(\phi) + D\cdot\sin(\phi) \tag{12}$$

$$dF_{tan} = L\cdot\sin(\phi) - D\cdot\cos(\phi) \tag{13}$$

$$\text{Power} = \Omega\int_{r_{hub}}^{R} dF_{tan} r dr \tag{14}$$

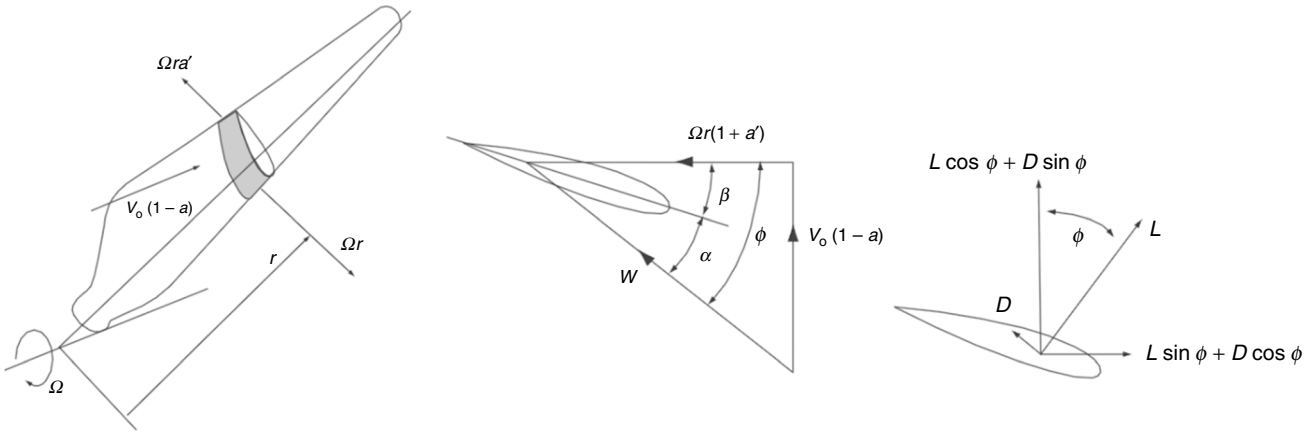

Fig. 1 Arrangement of how to analyze the blade elements

$$\mathrm{TSR} = \frac{\Omega R}{V_o} \tag{15}$$

c is chord length in Eqs. (10) and (11), dF_{ax} and dF_{tan} are axial and tangential induced forces on the element length in Eqs. (12) and (13) respectively, R and r_{hub} are tip and hub radius of the rotor in Eq. (14), Power is output power generated by the rotor in Eq. (14), and TSR is tip speed ratio of the rotor in Eq. (15).

3D modeling for the stall region

The BEM theory is a 1D code, which is not able to take into account the 3D flows effect aerodynamics of blades. An aerofoil data correction described by [47] was used in this study to convert lift confident of aerofoil data from two dimensions to three dimensions.

$$C_{l,3D} = C_{l,2D} + x\left(\frac{c}{r}\right)^{y} \cos^4(\phi)\left(C_{l,\,inv} - C_{l,\,2D}\right) \tag{16}$$

Figure 2 describes how to alter the lift coefficients. By extending the linear part of the origin curve (in viscid part), the stall region will be covered. The difference between two curves $\Delta C_l = C_{l,inv} - C_{l,2D}$ is multiplied by $x(c/r)y$, where $x = 2.2$ and $y = 1$ according to [39].

Methodology

As it shown in Fig. 3, the following steps are taken to obtain the output results of BEM based on C programming.

Exergy modeling

The exergy concept depicts the locations of energy destruction in a process [53]. Therefore, the output result of exergy analysis can lead to enhance system operation [54]. Also, it can quantify the quality of energy in a thermodynamical process [55]. Exergy is the maximum work output generated by a system or a flow of matter or energy that has equilibrium with reference environmental conditions [56, 57]. In real process (except for ideal, or reversible processes), exergy is not subject to a conservation law and it will be consumed or destroyed, due to the irreversibilities of process [58]. In exergy analysis, the characteristics of a reference environment must be specified [59]. It can be done by specifying the variables namely pressure, relative humidity, temperature, and chemical composition of the reference environment. Therefore, the output results are rely on the specified reference environment [60].

In this section, the modeling of both energy efficiency (η) (Eq. 17) and the exergy efficiency (Ψ) (Eq. 18) for the wind turbine are described. Like the other thermodynamics systems having limitations in efficiency due to the irreversibility [61–63], it is not possible for the wind turbine to extract the total kinetic energy of the flow. Based on

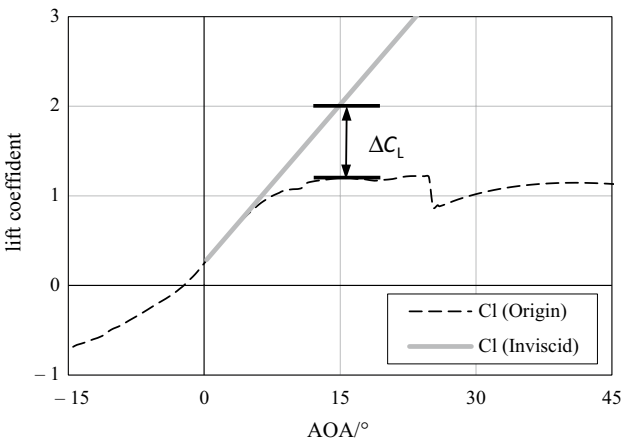

Fig. 2 The preparation of lift coefficients for 3D conversion

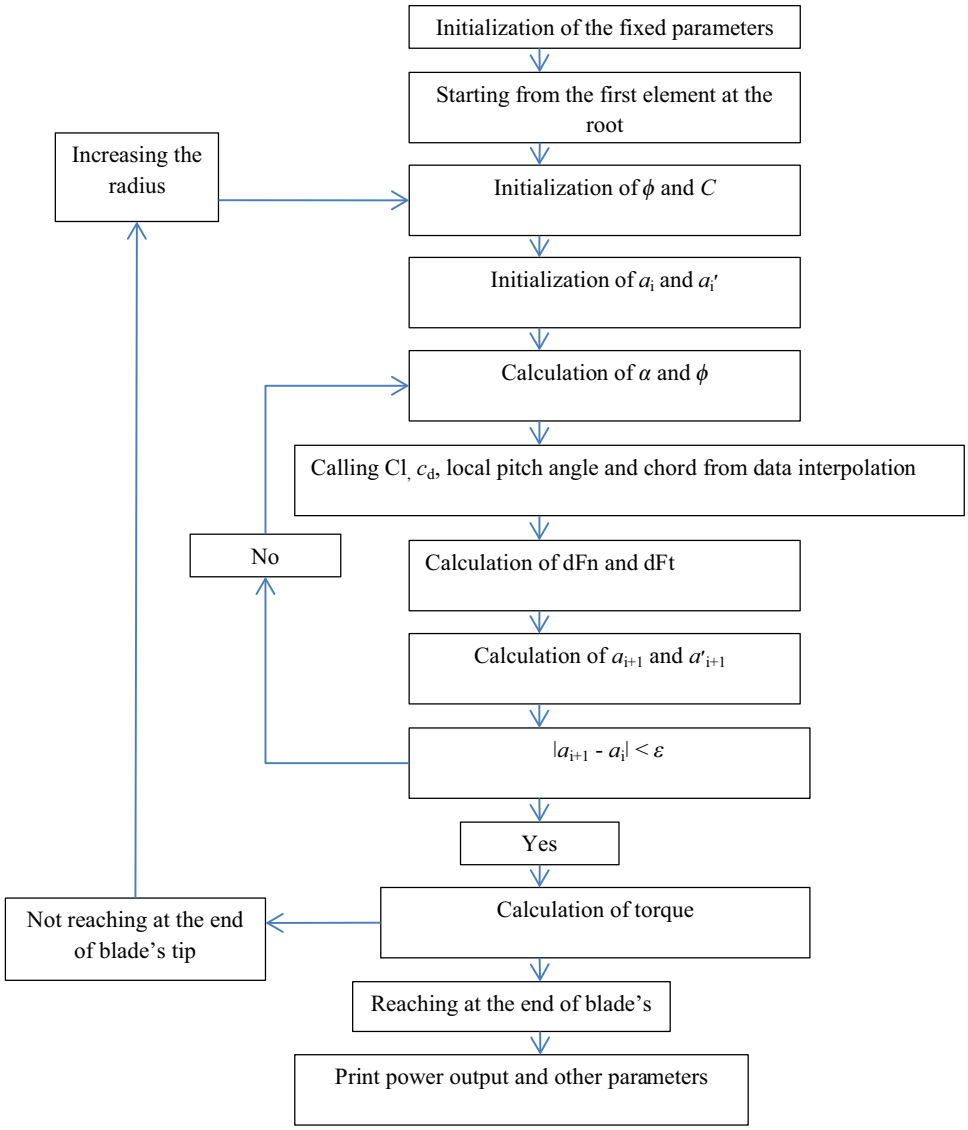

Fig. 3 Algorithm designed for the enhanced BEM method in the current study

Betz's law, wind turbines can convert less than 59% of the wind power to output power [64]. Nevertheless, in practice, their efficiency is about 40% for great wind speeds. The energy efficiency is the ratio of total useful work produced by a wind turbine to the difference in kinetic energy of wind flow. Also, the exergy efficiency is the proportion of useful work to the exergy of the wind passing through the wind turbine (see Fig. 4) [65].

$$\eta = \frac{W_{\text{out}}}{\text{kinetic energy of wind}} \tag{17}$$

$$\Psi = \frac{W_{\text{out}}}{\text{Ex}_{\text{flow}}} \tag{18}$$

The energy balance equation of the wind turbine is defined by [65]:

$$\text{ke}_1 = W_{\text{out}} + \text{ke}_2 \tag{19}$$

where $\text{ke}_{1,2}$ is the kinetic energy of wind flow before and after the wind rotor plan, respectively.

$$\text{ke}_{1,2} = \frac{1}{2}\dot{m}v_{1,2}^2 \tag{20}$$

The mass flow rate of the wind turbine can be introduced by:

$$\dot{m} = \rho\pi r^2 v \tag{21}$$

The output velocity of the wind turbine can be calculated by [28]:

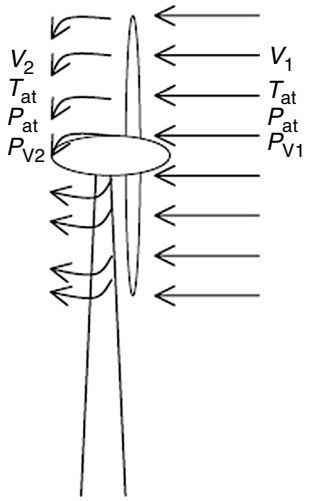

Fig. 4 The diagram of inlet and outlet parameters states in the rotor plan

$$v_2 = \sqrt[3]{\frac{2\left(\mathrm{ke}_1 - W_{\mathrm{out}}\right)}{\rho\pi R^2 t}} \tag{22}$$

The exergy balance for this model is [65]:

$$\mathrm{Ex}_{\mathrm{flow}} = \mathrm{Ex}_{\mathrm{ph}} + \mathrm{ke} \tag{23}$$

$$\mathrm{Ex}_{\mathrm{ph}} = m\left[c_{\mathrm{p}}\left(T_2 - T_1\right) + T_0\left(C_{\mathrm{P}} \ln\left(\frac{T_2}{T_1}\right) - R\ln\left(\frac{P_2}{P_1}\right) - \frac{C_{\mathrm{P}}(T_0 - T_{\mathrm{avg}})}{T_0}\right)\right] \tag{24}$$

And the wind turbine's destruction can be defined by [66]:

$$\mathrm{EX}_{\mathrm{des}} = T_0\left(C_P \ln\left(\frac{T_2}{T_1}\right) - R\ln\left(\frac{P_2}{P_1}\right) - \frac{C_{\mathrm{P}}(T_0 - T_{\mathrm{avg}})}{T_0}\right) \tag{25}$$

where $P_{1,2} = P_0 \pm (\rho/2)(V_{1,2})^2$. Also, the temperatures of flow in both states $T_{1,2}$ are calculated through the wind chill temperature formula developed in [67].

$$T_{\mathrm{windch}} = 13.12 + 0.6215T_{\mathrm{at}} - 11.37V^{0.16} + 0.3965T_{\mathrm{at}}V^{0.16} \tag{26}$$

Finally, Eq. (27) can be used for exergy of humid air [26].

$$\mathrm{Ex}_{\mathrm{ph}} = m\left[\left(c_{\mathrm{p.a}} + \varpi C_{\mathrm{p.v}}\right)\left(T - T_0\right) - T_0\left[\left(c_{\mathrm{p.a}} + \varpi C_{\mathrm{p.v}}\right)\ln\left(\frac{T}{T_0}\right) - \left(R_{\mathrm{a}} + \varpi R_{\mathrm{v}}\right)\ln\left(\frac{P}{P_0}\right)\right] + T_0\left[\left(R_{\mathrm{a}} + \varpi R_{\mathrm{v}}\right)\ln\left(\frac{1 + 1.6078\varpi_0}{1 + 1.6078\varpi}\right) + 1 + 1.6078R_{\mathrm{a}}\varpi\ln\left(\frac{\varpi}{\varpi_0}\right)\right]\right] \tag{27}$$

Fig. 5 INER-P150II wind turbine

Table 1 the specification of nominated wind turbine [68]

Rated RPM	45–50
Cut-in wind speed	3 m s^{-1}
Cut-out wind speed	25 m s^{-1}
Hub height	50 m

In this research, the reference pressure and temperature are taken based on the experiment environmental condition (101.3 kPa and 298 K), respectively.

Case study

A horizontal-axis and a three-bladed wind turbine with a 150 KW power output named INER-P150II is used in this study [68] (see Fig. 5). The pitch angle and chord length are varied along the wind blade with 10.8 m length. Moreover, different types of airfoil sections such as DU series, NACA0013166, and FX63-137 were used from the root to tip blade. The wind turbine specification is summarized in Table 1.

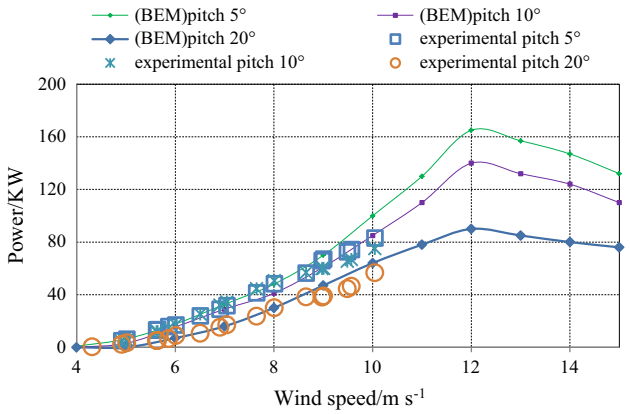

Fig. 6 Comparison of output power between BEM model and experimental data under

Results and discussion

One important reason to implement the BEM method in this study is that to achieve clear anticipation about the power productions and power calculating the wind speed behind the rotor plan. The results of the output power under different speeds and pitch angles are presented and compared with experimental data in Fig. 6. With increasing the wind speed from 5 to 12 m s^{-1}, the power production of the wind turbine increases steadily; however, after peaking at 12 m s^{-1} there is a reduction in the power production for all three modelings. Also, the results of the BEM modeling are almost in the same phase with experimental data in low wind speed under 10 m s^{-1}. It is anticipated that the wind turbine can produce 165 KW output power under the wind speed of 12 m s^{-1} and pitch angle of 5°. Also, it is shown that increasing the pitch angle will decrease the power production more specificity in high wind speeds.

As seen in Fig. 7, both energy and exergy efficiencies of the wind turbine are increased by rising the wind speed from 5 to 12 m s^{-1} at the pitch angle of 5° and 10°, while in higher wind speeds up to 12 m s^{-1} the wind turbine has faced with a steady reduction in efficiency. The maximum exergy and energy efficiencies are 42.8% and 43.9% at wind speed 12 m s^{-1} and pitch angle 5°. Moreover, the wind turbine has had the lowest efficiency at pitch angle 20° compared to other pitch angles. Also, it should be mentioned that since the energy analysis just shows changing the kinetic energy and is not able to depict the effects of the temperature, pressure, and humidity, it predicts the higher efficiency more than the exergy efficiency.

Wind speed is the most important source of the exergy flow in the wind systems; however, the wind turbine is not able to extract all of the wind exergy and the leftover of the upcoming wind leave the rotor plan and disappear. Also, due to the wake production behind the wind blades in both laminar and turbulent flows as main sources of entropy production, the amount of the exergy destruction is shown in this study. As seen in Fig. 8, while wind speed increases, both exergy destruction and exergy flow rise continuously. By increasing the pitch angle from 5° to 20°, the wind blade will touch the higher angle of attacks, which means that the flow separation behind the blade will increase considerably. Therefore, it increases the wake production in the flow stream behind the wind turbine; consequently, the exergy destruction will increase dramatically.

Regarding the former figures, it is shown that wind speed has a noticeable effect on the wind turbine's performance, but in figures from 9 to 11 it will show the effect of the other metrological parameters on the exergy efficiency in four wind speeds of 8, 10, 12, and 14 m s^{-1} and three pitch angles of 5°, 10° and 20°. As seen in Fig. 9 increasing the relative humidity has had a negative effect on the exergy efficiency in all three pitch angles; however, this impact on the higher wind speeds (12 and 14 m s^{-1}) is not very sensible. By increasing the pitch angle, this amount of the reduction increases too. The higher exergy efficiency loss has occurred at the wind speed of 8 m s^{-1} and pitch angle 20° (near 1.76%), When the relative humidity increases from 0.001 to 0.015.

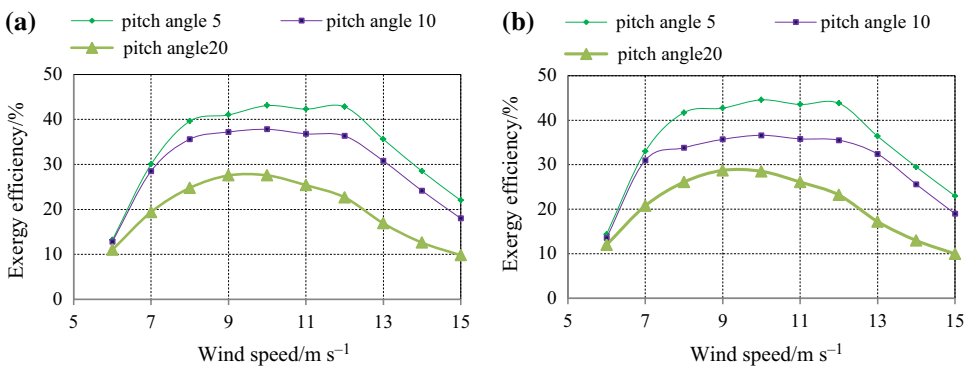

Fig. 7 **a** Exergy efficiency. **b** Energy efficiency of the wind turbine against the wind speed in various pitch angles

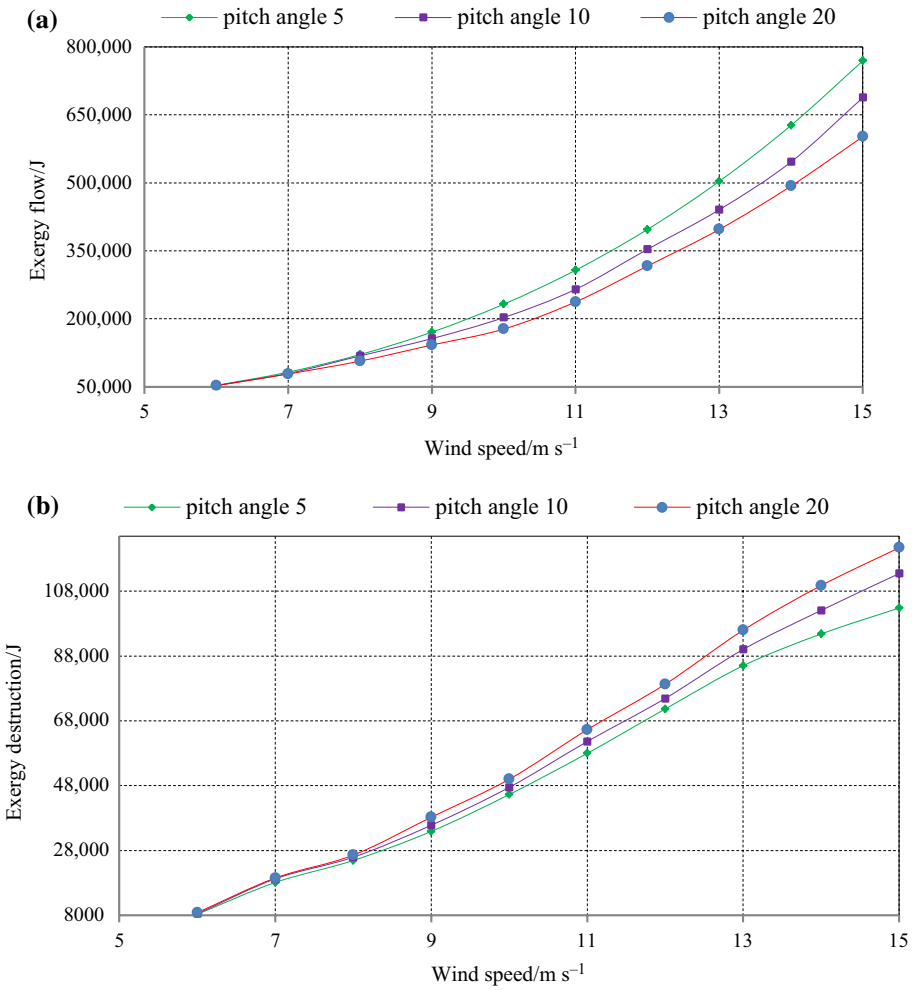

Fig. 8 Compression of the **a** exergy flow and **b** exergy destruction under different wind speeds

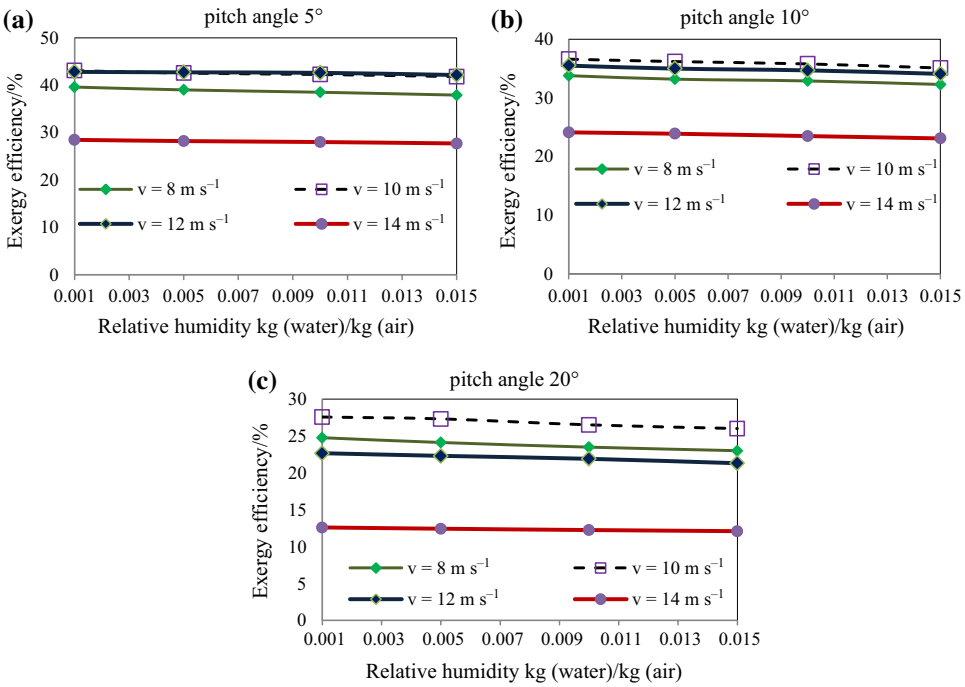

Fig. 9 Effect of relative humidity on exergy efficiency in different wind speed. **a** Pitch angle 5°. **b** Pitch angle 10°. **c** Pitch angle 20°

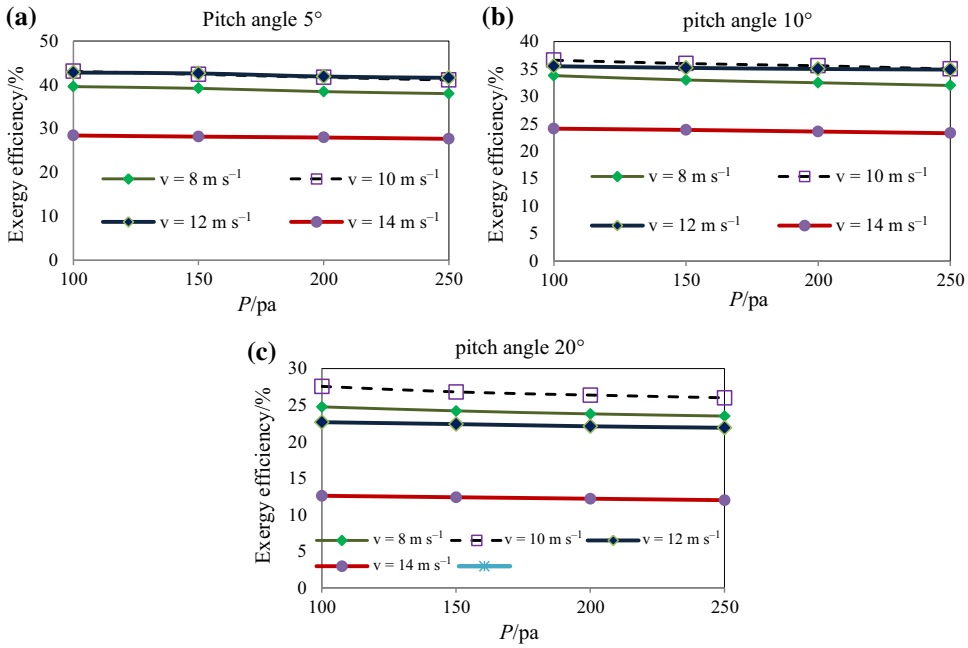

Fig. 10 Effect of pressure changing on exergy efficiency in different wind speed. **a** Pitch angle 5°. **b** Pitch angle 10°. **c** Pitch angle 20°

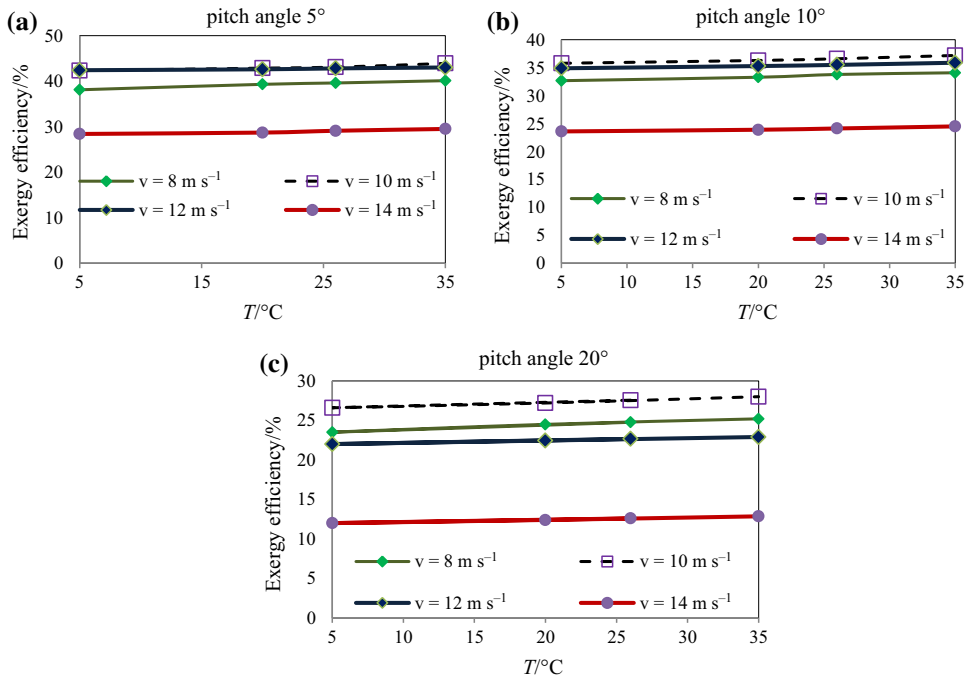

Fig. 11 Effect of temperature on exergy efficiency in different wind speed. **a** Pitch angle 5°. **b** Pitch angle 10°. **c** Pitch angle 20°

In Fig. 10, the relation between pressure changes (from 100 to 250 pa) and exergy efficiency is shown. Likely, changing the Δp from 100 to 240 pa has had an adverse effect on the exergy efficiency, especially at the lower speeds and pitch angle 20°. In wind speeds more than 10 m s^{-1}, the effect of the wind speed on the wind turbine's efficiency is dominant. Therefore, the sensibility of the system to other parameters becomes insignificant. It is shown that by increasing the pressure changes from 100 to 250 pa at the wind speed of 8 m s^{-1} and pitch angle of 20° the exergy efficiency will decrease 1.26%.

Numerical evaluation between changing the ambient temperature and exergy efficiency is depicted in Fig. 11. Compared to pressure changing and relative humidity, the temperature has a straight effect on exergy efficiency. In all three pitch angles, temperature has had the highest effect on the wind speed of 8 m s^{-1}. It is shown that by increasing the ambient temperature from 5 to 35 °C, exergy efficiency

increases from 38.1 to 40.1% in wind speed of 8 m s^{-1} and pitch angle 5°.

Conclusions

In this study, the wind turbine's performance in different conditions based on the energy and exergy analysis is studied.

- The BEM code has had a good agreement with experimental data to calculate the power production for all three pitch angles.
- The maximum exergy and energy efficiencies are 42.8% and 43.9% at wind speed 12 m s^{-1} and pitch angle 5°
- Wind speed has the highest impact on the energy and exergy efficiency of the wind turbine, compared to the temperature, pressure changes and relative humidity.
- Temperature has a positive effect on the exergy efficiency and by increasing the temperature from 5 to 35 °C, the exergy efficiency rises 2% at the wind speed of 8 m s^{-1} and pitch angle of 5°,
- Increasing the relative humidity from 0.001 to 0.015 and pressure changes from 100 to 240 pa can decrease the exergy efficiency 1.76% and 1.26% at the wind speed of 8 m s^{-1} and pitch angle of 20°, respectively.
- Effects of the pressure, temperature and relative humidity in the low wind speeds (less than 10 m s^{-1}) are more significant than the high wind speeds on the wind turbine.

References

1. Kaushik SC, Singh OK. Estimation of chemical exergy of solid, liquid and gaseous fuels used in thermal power plants. J Therm Anal Calorim. 2014;115:903–8. https://doi.org/10.1007/s10973-013-3323-9.
2. Javadi MA, Hoseinzadeh S, Ghasemiasl R, Heyns PS, Chamkha AJ. Sensitivity analysis of combined cycle parameters on exergy, economic, and environmental of a power plant. J Therm Anal Calorim. 2020;139:519–25. https://doi.org/10.1007/s10973-019-08399-y.
3. Kalbasi R, Izadi F, Talebizadehsardari P. Improving performance of AHU using exhaust air potential by applying exergy analysis. J Therm Anal Calorim. 2020;139:2913–23. https://doi.org/10.1007/s10973-019-09198-1.
4. Naeimi A, Bidi M, Ahmadi MH, Kumar R, Sadeghzadeh M, Alhuyi Nazari M. Design and exergy analysis of waste heat recovery system and gas engine for power generation in Tehran cement factory. Therm Sci Eng Prog. 2019;9:299–307. https://doi.org/10.1016/j.tsep.2018.12.007.
5. Mohammadi A, Kasaeian A, Pourfayaz F, Ahmadi MH. Thermodynamic analysis of a combined gas turbine, ORC cycle and absorption refrigeration for a CCHP system. Appl Therm Eng. 2017;111:397–406. https://doi.org/10.1016/j.applthermaleng.2016.09.098.
6. Ahmadi MH, Ghazvini M, Sadeghzadeh M, Alhuyi Nazari M, Ghalandari M. Utilization of hybrid nanofluids in solar energy applications: a review. Nano-Struct Nano-Objects. 2019;20:100386. https://doi.org/10.1016/j.nanoso.2019.100386.
7. Ahmadi MH, Sayyaadi H, Mohammadi AH, Barranco-Jimenez MA. Thermo-economic multi-objective optimization of solar dish-stirling engine by implementing evolutionary algorithm. Energy Convers Manag. 2013;73:370–80. https://doi.org/10.1016/j.enconman.2013.05.031.
8. Zachar M, Lieskovský M, Majlingová A, Mitterová I. Comparison of thermal properties of the fast-growing tree species and energy crop species to be used as a renewable and energy-efficient resource. J Therm Anal Calorim. 2018;134:543–8. https://doi.org/10.1007/s10973-018-7194-y.
9. Ren21. The first decade: 2004–2014, 10 years of renewable energy progress; 2014 2004–2014. doi: 9783981593440.
10. Ahmadi MH, Mehrpooya M, Pourfayaz F. Thermodynamic and exergy analysis and optimization of a transcritical CO2 power cycle driven by geothermal energy with liquefied natural gas as its heat sink. Appl Therm Eng. 2016;109:640–52. https://doi.org/10.1016/j.applthermaleng.2016.08.141.
11. Naseri A, Bidi M, Ahmadi MH. Thermodynamic and exergy analysis of a hydrogen and permeate water production process by a solar-driven transcritical CO2 power cycle with liquefied natural gas heat sink. Renew Energy. 2017;113:1215–28. https://doi.org/10.1016/j.renene.2017.06.082.
12. Ahmadi MH, Ahmadi MA, Bayat R, Ashouri M, Feidt M. Thermo-economic optimization of Stirling heat pump by using non-dominated sorting genetic algorithm. Energy Convers Manag. 2015;91:315–22. https://doi.org/10.1016/j.enconman.2014.12.006.
13. Caruso C, Catenacci G, Marchettini N, Principi I, Tiezzi E. Emergy based analysis of Italian electricity production system. J Therm Anal Calorim. 2001. https://doi.org/10.1023/a:1012412420744.
14. Ahmadi MH, Alhuyi Nazari M, Sadeghzadeh M, Pourfayaz F, Ghazvini M, Ming T, Meyer JP, Sharifpur M. Thermodynamic and economic analysis of performance evaluation of all the thermal power plants: a review. Energy Sci Eng. 2019;7:30–65. https://doi.org/10.1002/ese3.223.
15. Namar MM, Jahanian O. Energy and exergy analysis of a hydrogen-fueled HCCI engine. J Therm Anal Calorim. 2019;137:205–15. https://doi.org/10.1007/s10973-018-7910-7.
16. Tian C, Maleki A, Motie S, Yavarinasab A, Afrand M. Generation expansion planning by considering wind resource in a competitive environment. J Therm Anal Calorim. 2020;139:2847–57. https://doi.org/10.1007/s10973-019-09139-y.
17. Gu Q, Ren H, Gao W, Ren J. Integrated assessment of combined cooling heating and power systems under different design and management options for residential buildings in Shanghai. Energy Build. 2012;51:143–52. https://doi.org/10.1016/j.enbuild.2012.04.023.
18. Barhoumi EM, Okonkwo PC, Zghaibeh M, Ben Belgacem I, Alkanhal TA, Abo-Khalil AG, Tlili I. Renewable energy resources and workforce case study Saudi Arabia: review and recommendations. J Therm Anal Calorim. 2019. https://doi.org/10.1007/s10973-019-09189-2.
19. Koroneos C, Spachos T, Moussiopoulos N. Exergy analysis of renewable energy sources. Renew Energy. 2003;28:295–310.
20. Khalilzadeh S, Hossein Nezhad A. Utilization of waste heat of a high-capacity wind turbine in multi effect distillation desalination: energy, exergy and thermoeconomic analysis. Desalination. 2018;439:119–37. https://doi.org/10.1016/j.desal.2018.04.010.
21. Nematollahi O, Hajabdollahi Z, Hoghooghi H, Kim KC. An evaluation of wind turbine waste heat recovery using organic

Rankine cycle. J Clean Prod. 2019;214:705–16. https://doi.org/10.1016/j.jclepro.2019.01.009.
22. Khosravi A, Koury RNN, Machado L, Pabon JJG. Energy, exergy and economic analysis of a hybrid renewable energy with hydrogen storage system. Energy. 2018;148:1087–102. https://doi.org/10.1016/j.energy.2018.02.008.
23. Mohammadi A, Ahmadi MH, Bidi M, Joda F, Valero A, Uson S. Exergy analysis of a combined cooling, heating and power system integrated with wind turbine and compressed air energy storage system. Energy Convers Manag. 2017;131:69–78. https://doi.org/10.1016/j.enconman.2016.11.003.
24. Aghbashlo M, Tabatabaei M, Hosseini SS, Dashti BB, Mojarab Soufiyan M. Performance assessment of a wind power plant using standard exergy and extended exergy accounting (EEA) approaches. J Clean Prod. 2018;171:127–36. https://doi.org/10.1016/j.jclepro.2017.09.263.
25. Ahmadi EMA. Exergy analysis of a wind turbine. Int J Exergy. 2009;6:457–76.
26. Baskut O, Ozgener O, Ozgener L. Effects of meteorological variables on exergetic efficiency of wind turbine power plants. Renew Sustain Energy Rev. 2010;14:3237–41. https://doi.org/10.1016/j.rser.2010.06.002.
27. Pope K, Dincer I, Naterer GF. Energy and exergy efficiency comparison of horizontal and vertical axis wind turbines. Renew Energy. 2010;35:2102–13. https://doi.org/10.1016/j.renene.2010.02.013.
28. Khanjari A, Sarreshtehdari A, Mahmoodi E. Modeling of energy and exergy efficiencies of a wind turbine based on the blade element momentum theory under different roughness intensities. J Energy Resour Technol. 2016;139:022006. https://doi.org/10.1115/1.4034640.
29. Khanjari A, Mahmoodi E, Sarreshtehdari A, Chahartaghi M. Modelling of energy and exergy efficiencies of a horizontal axis wind turbine based on the blade element momentum theory at different yaw angles. Int J Exergy. 2018;27:437–59. https://doi.org/10.1504/ijex.2018.096002.
30. Keramat Siavash N, Najafi G, Tavakkoli Hashjin T, Ghobadian B, Mahmoodi E. An innovative variable shroud for micro wind turbines. Renew Energy. 2020;145:1061–72. https://doi.org/10.1016/j.renene.2019.06.098.
31. Bernabini L, Martinez J. An improved BEM model for the power curve prediction of stall-regulated wind turbines. Wind Energy. 2004;8:385–402.
32. Keramat Siavash N, Najafi G, Tavakkoli Hashjin T, Ghobadian B, Mahmoodi E. Mathematical modeling of a horizontal axis shrouded wind turbine. Renew Energy. 2020;146:856–66. https://doi.org/10.1016/j.renene.2019.07.022.
33. Boojari M, Mahmoodi E, Khanjari A. Wake modelling via actuator-line method for exergy analysis in openFOAM. Int J Green Energy. 2019;16:797–810. https://doi.org/10.1080/15435075.2019.1641101.
34. Mahmoodi E, Schaffarczyk AP. Actuator disc modeling of the MEXICO rotor experiment. Berlin: Springer; 2014. p. 29–34. https://doi.org/10.1007/978-3-642-54696-9_5.
35. Sørensen JN, Shen WZ, Munduate X. Analysis of wake states by a full-field actuator disc model. Wind Energy. 1998;1:73–88. https://doi.org/10.1002/(sici)1099-1824(199812)1:2%3c73:aid-we12%3e3.0.co;2-l.
36. Sanderse B, Pijl SP, Koren B. Review of computational fluid dynamics for wind turbine wake aerodynamics. Wind Energy. 2011;14:799–819. https://doi.org/10.1002/we.458.
37. Naderi S, Torabi F. Numerical investigation of wake behind a HAWT using modified actuator disc method. Energy Convers Manag. 2017;148:1346–57. https://doi.org/10.1016/j.enconman.2017.07.003.
38. Khanjari A, Mahmoodi E, Sarreshtehdari A. Effect of stall delay model on momentum distribution of wind turbine' s blade under yaw condition: compared to MEXICO experiment. Iran J Energy Environ. 2018;9:16–23. https://doi.org/10.5829/ijee.2018.09.01.03.
39. Mahmoodi E, Jafari A, Peter Schaffarczyk A, Keyhani A, Mahmoudi J. A new correlation on the MEXICO experiment using a 3D enhanced blade element momentum technique. Int J Sustain Energy. 2013;1:13. https://doi.org/10.1080/14786451.2012.759575.
40. Syed Ahmed Kabir IF, Ng EYK. Insight into stall delay and computation of 3D sectional aerofoil characteristics of NREL phase VI wind turbine using inverse BEM and improvement in BEM analysis accounting for stall delay effect. Energy. 2017;120:518–36. https://doi.org/10.1016/j.energy.2016.11.102.
41. Pinto RLUDF, Gonçalves BPF. A revised theoretical analysis of aerodynamic optimization of horizontal-axis wind turbines based on BEM theory. Renew Energy. 2017;105:625–36. https://doi.org/10.1016/j.renene.2016.12.076.
42. Arramach J, Boutammachte N, Bouatem A, Al Mers A. Prediction of the wind turbine performance by using a modified BEM theory with an advanced brake state model. Energy Procedia. 2017;149:157. https://doi.org/10.1016/j.egypro.2017.07.033.
43. Zhong W, Shen WZ, Wang T, Li Y. A tip loss correction model for wind turbine aerodynamic performance prediction. Renew Energy. 2020;147:223–38. https://doi.org/10.1016/j.renene.2019.08.125.
44. Froude W. On the elementary relation between pitch, slip and propulsive efficiency. Trans Inst Nav Archit. 1878;19:47–57.
45. Glauert H. Airplane propellers, Division L. Julius. Springer, New York; 1935. http://link.springer.com/chapter/10.1007/978-3-642-91487-4_3. Accessed 18 Dec 2015.
46. Sørensen J. Aerodynamic aspects of wind energy conversion. Annu Rev Fluid Mech. 2011;43:427–48.
47. Hansen MOL. Aerodynamics of wind turbines. 2nd ed. New York: Wiley; 2008. https://doi.org/10.1002/0470846127.
48. Rankine W. On the mechanical principles of the action of propellers. Trans Inst Nav Archit. 1865;6:13–39.
49. Froude R. On the part played in propulsion by differences of fluid pressure. Trans Inst Nav Archit. 1889;30:390–423.
50. Hernandez J, Crespo A. Aerodynamics calculation of the performance of horizontal axis wind turbines and comparison with experimental results. Wind Eng. 1987;11:177–87.
51. Moriarty P, Hansen A. AeroDyn theory manual. National Renewable Energy Laboratory, colorado; 2005. http://www.nrel.gov/docs/fy05osti/36881.pdf. Accessed 22 Dec 2015.
52. Wilson R. Fundamental concepts in wind turbine engineering. In: Spera DA. 2 ed. ASME, New York; 2009. http://gasturbinespower.asmedigitalcollection.asme.org/pdfAccess.ashx?url=%252Fdata%252FBooks%252F802601%252F802601_ch5a.pdf. Accessed 22 Dec 2015.
53. Kumar AKBA, Nikam KC. An exergy analysis of a 250 MW thermal power plant. Renew Energy Res Appl. 2020;1:197–204. https://doi.org/10.22044/rera.2020.9460.1025.
54. Nouri M, Namar MM, Jahanian O. Analysis of a developed Brayton cycled CHP system using ORC and CAES based on first and second law of thermodynamics. J Therm Anal Calorim. 2019;135:1743–52. https://doi.org/10.1007/s10973-018-7316-6.
55. Akbari Vakilabadi M, Bidi M, Najafi AF, Ahmadi MH. Energy, exergy analysis and performance evaluation of a vacuum evaporator for solar thermal power plant zero liquid discharge systems. J Therm Anal Calorim. 2020;139:1275–90. https://doi.org/10.1007/s10973-019-08463-7.
56. Senturk Acar M, Arslan O. Energy and exergy analysis of solar energy-integrated, geothermal energy-powered organic Rankine cycle. J Therm Anal Calorim. 2019;137:659–66. https://doi.org/10.1007/s10973-018-7977-1.

57. Kalbasi R, Shahsavar A, Afrand M. Incorporating novel heat recovery units into an AHU for energy demand reduction-exergy analysis. J Therm Anal Calorim. 2019;139:2821–30. https://doi.org/10.1007/s10973-019-09060-4.
58. Bagherzadeh SA, Ruhani B, Namar MM, Alamian R, Rostami S. Compression ratio energy and exergy analysis of a developed Brayton-based power cycle employing CAES and ORC. J Therm Anal Calorim. 2020;139:2781–90. https://doi.org/10.1007/s10973-019-09051-5.
59. Ayub I, Munir A, Amjad W, Ghafoor A, Nasir MS. Energy- and exergy-based thermal analyses of a solar bakery unit. J Therm Anal Calorim. 2018;133:1001–13. https://doi.org/10.1007/s10973-018-7165-3.
60. Paradeshi L, Mohanraj M, Srinivas M, Jayaraj S. Correction to: Exergy analysis of direct-expansion solar-assisted heat pumps working with R22 and R433A. J Therm Anal Calorim. 2018;134(3): 2223–2237. https://doi.org/10.1007/s10973-018-7424-3, J Therm Anal Calorim. 2018;134:2239. https://doi.org/10.1007/s10973-018-7751-4.
61. Ahmadi MH, Ahmadi MA, Mellit A, Pourfayaz F, Feidt M. Thermodynamic analysis and multi objective optimization of performance of solar dish Stirling engine by the centrality of entransy and entropy generation. Int J Electr Power Energy Syst. 2016;78:88–95. https://doi.org/10.1016/j.ijepes.2015.11.042.
62. Sadatsakkak SA, Ahmadi MH, Ahmadi MA. Thermodynamic and thermo-economic analysis and optimization of an irreversible regenerative closed Brayton cycle. Energy Convers Manag. 2015;94:124–9. https://doi.org/10.1016/j.enconman.2015.01.040.
63. Ahmadi MH, Ahmadi MA, Mehrpooya M, Sameti M. Thermo-ecological analysis and optimization performance of an irreversible three-heat-source absorption heat pump. Energy Convers Manag. 2015;90:175–83. https://doi.org/10.1016/j.enconman.2014.11.021.
64. Betz A. Das Maximum der theoretisch moeglichen Ausnuetzung des Windes durch Windmotoren; 1920.
65. Dincer I, Rosen M. Exergy: energy, environment and sustainable development. 1st ed. Elsevier Science, Amsterdam; 2007. https://scholar.google.com/scholar?hl=en&q=I.+Dincer%252C+M.+A.+Rosen%252C+Exergy%253A+energy%252C+environment+and+sustainable+development%252C+1+ed.%252C+pp.+187-188%252C+Burlington%253A+Elsevier%252C+2007&btnG=&as_sdt=1%252C5&as_sdtp=#0. Accessed 22 Dec 2015.
66. Rosen A, Wolf A, Shmuel D, Omri G. Part 2. the Mexico project wind turbine model; 2011:287–301. https://scholar.google.com/scholar?q=Rosen%252C+A.%252C+Wolf%252C+A.%252C+Ben+Shmuel%252C+D.%252C+Omri%252C+G.%252C+2011a.+Part+I.+The+Mexico+project+wind+turbine+model.+IACAS%252C+Haifa&btnG=&hl=en&as_sdt=0%252C5#0. Accessed 22 Dec 2015.
67. Bluestein M, Zecher J. A new approach to an accurate wind chill factor. Bull Am Meteorol Soc. 1999;80:1893–9.
68. Lin YT, Chiu PH, Huang CC. An experimental and numerical investigation on the power performance of 150 kW horizontal axis wind turbine. Renew Energy. 2017;113:85–93. https://doi.org/10.1016/j.renene.2017.05.065.